Application of stress intensity factor superposition in residual stress fields considering crack closure

Keller, Sören; Klusemann, Benjamin

Published in:
Engineering Fracture Mechanics

DOI:
10.1016/j.engfracmech.2020.107415

Publication date:
2021

Document Version
Publisher's PDF, also known as Version of record

Engineering Fracture Mechanics 243 (2021) 107415

Contents lists available at ScienceDirect

Engineering Fracture Mechanics

journal homepage: www.elsevier.com/locate/engfracmech

Application of stress intensity factor superposition in residual stress fields considering crack closure

S. Keller [a,*], B. Klusemann [a,b]

[a] Helmholtz-Zentrum Geesthacht, Institute of Materials Research, Materials Mechanics, Max-Planck-Straße 1, 21502 Geesthacht, Germany
[b] Leuphana University of Lüneburg, Institute of Product and Process Innovation, Universitätsallee 1, 21335 Lüneburg, Germany

ARTICLE INFO

Keywords:
Stress intensity factor
Residual stress
Superposition principle
Crack closure

ABSTRACT

The correlation between stress intensity factor (SIF) range and fatigue crack growth is a powerful tool for fail-safe design approaches applied to lightweight structures. The key role is precise calculation of the SIFs of fatigue load cycles. Advanced material processing can shape residual stresses and makes SIF calculation a challenging task. While the consideration of tensile residual stresses is successfully tackled by SIF superposition, the treatment of compressive residual stresses needs still clarification. This work demonstrates the application of the SIF superposition principle in regions containing high compressive residual stresses leading to crack closure effects. Crack closure depends on the combined load of residual and applied stresses and is interpreted as a change of crack geometry in this work. Thus the relation between the source, i.e. the applied or residual stress, and its consequence, i.e. the corresponding SIFs, depends on the interaction of the sources, i.e. the combined load. Due to this interaction, residual stress-induced changes of the fatigue behaviour cannot be linked to the residual or applied SIF only. This work proposes two alternative definitions of applied and residual SIF, allowing a clear correlation between either residual or applied SIF to fatigue behaviour changes.

1. Introduction

The precise estimation of fatigue crack growth (FCG) is an important issue in design and maintenance of metallic lightweight structures. Especially the knowledge of the fatigue crack growth rate (FCGR) leads to an optimization of inspection intervals which is of high economic interest. It is known that the FCGR can be significantly influenced by residual stresses [1,2], especially when the ratio of residual and applied stresses is high [3]. Therefore, several residual stress modification techniques, allowing the generation of tailored residual stress profiles, e.g. hammer peening [4], shot peening [5], or laser shock peening [6], are applied to fatigue critical components. While tensile residual stresses are supposed to accelerate FCG, compressive residual stresses can cause beneficial FCG retardation [1]; however, the favourable compressive residual stresses are always accompanied by balancing tensile stresses. Therefore, exact knowledge of the residual stress field and tools for the estimation of the FCGR influenced by residual stresses are necessary to extend the inspection intervals without compromising safety aspects.

A common approach to estimate FCGR in sheet-like structures is the calculation of stress intensity factors (SIFs), which are successively applied to empirical FCG equations such as Paris' law [7] or NASGRO Eq. [8]. Typical inputs of these FCG equations are the SIF range and/or SIF ratio under the fatigue load cycles. Elber [9] related a lower FCGR to crack closure effects located next to the crack front that reduce the SIF range. This crack closure is caused by plastic deformation of the material next to the fracture surfaces, also named as

* Corresponding author.
E-mail address: soeren.keller@hzg.de (S. Keller).

https://doi.org/10.1016/j.engfracmech.2020.107415
Received 13 May 2020; Received in revised form 17 September 2020; Accepted 10 November 2020
Available online 11 December 2020

plastic wake, originally introduced by the stress field next to the crack front. This type of crack closure phenomenon is know as *plasticity induced* crack closure. The proposed solution is the correction of the SIF range to an effective SIF range. The correction is typically expressed with a crack opening function, such as proposed by Newman [10]. Residual stresses, introduced via local modification techniques, are based on the generation of plastic strain gradients. Therefore, crack closure caused by such residual stresses during FCG can be interpreted as *plasticity induced* as well. The difference of crack closure in compressive residual stress fields and Elber's *plasticity induced* crack closure is the origin of plastic deformation. In theory, crack opening functions for specific compressive residual stress fields could be found as well. However, residual stress modification techniques allow specific shaping of stress fields, where it is impracticable to determine crack opening functions for theoretically all arbitrary residual stress profiles. Furthermore, it is shown by our previous work [11] that specific residual stress fields change the areas of crack closure, which are not necessarily connected to the crack front.

In the context of linear elastic fracture mechanics, the influence of residual stresses on the actual SIF can be interpreted as a superposition of a residual SIF K_{res} caused by residual stresses and an applied SIF K_{appl} resulting from applied loadings leading to $K_{tot} = K_{appl} + K_{res}$, see e.g. [12–14], where the total SIF K_{tot} approximates the actual SIF. This concept is experimentally validated by Newman et al. [15] when no crack closure occurs. However, crack closure leads to a non-linear relation between the applied loading and the total SIF. Some authors assume that a negative total SIF resulting from the superposition is not valid [16–19] and replace negative total SIF by zero ($K_{tot} = 0$, if $K_{appl} + K_{res} < 0$ MPa$\sqrt{\text{mm}}$). This method is also called *modified superposition method*. A direct consideration of crack closure is added in the *superposition contact method* [20] and the *new superposition contact method* [21]. In the latter one, a third SIF K_{cp} caused by contact pressure at the crack surfaces is added to the superposition of residual and applied SIFs $K_{tot} = K_{appl} + K_{res} + K_{cp}$. While the *superposition contact method* allows a negative total SIF, the *new superposition contact method* replaces a negative total SIF by zero, similar to the *modified superposition method*. However, the question of the residual SIF calculation arises for all superposition techniques, e.g. if residual stress redistribution due to the crack growth needs to be considered as investigated by Lam and Lian [22]. The physical meaning of the residual SIF depends on the applied method for the SIF superposition. However, the physical meaning of the residual SIF should be generalized, which needs further elaboration. Additionally, these methods for SIF superposition rely typically still on two-dimensional calculations. However, to account for high residual stress gradients through-the-thickness, for instance generated by laser shock peening, the model framework needs to be three-dimensional. Such residual stress gradients may lead to a partially opened crack front which is closed next to the surfaces due to compression and opened at material mid-thickness, where balancing tensile residual stresses are present, as experimentally and numerically shown in our previous work [11].

In this paper, the applicability of the superposition principle by interpreting crack closure phenomena as a change of the crack geometry is discussed from theoretical point of view and proofed by three-dimensional numerical simulations considering the residual stress redistribution due to the crack growth. It is shown, that crack closure changes the linear relation between loading and SIF in an elastic body, which can be interpreted as a change of the crack geometry. This interpretation follows the superposition of stresses in an elastic body and avoids the calculation of a SIF caused by crack surface tractions, which are interpreted as inner forces instead. The decomposition of the total SIF changes depending on the occurrence of crack closure and the related crack geometry, where both, the applied and the residual SIF depend on the occurrence of crack closure. The source of plastic deformation, causing the residual stresses and crack closure, does not influence the proposed interpretation of the SIF superposition. The authors think that a definition of a residual and an applied SIF should serve the precise discussion of the impact of residual stresses, therefore two different definitions of applied and residual SIFs are given and discussed regarding their physical meaning, simplifying the link between physical phenomenon, such as FCG, and applied as well as residual SIF.

2. SIF calculation and superposition

2.1. SIF calculation in residual stress-free material

Given the assumption that the plastic zone at the crack front during fatigue load is relatively small, linear elastic fracture mechanics is applied. For a two-dimensional problem, a SIF K can be correlated with the external loading F_{appl} via

$$K = Y F_{appl}, \tag{1}$$

where Y is a geometry factor. Residual stresses are not considered. According to ASTM E647-15 the geometry factor Y of a C(T) specimen is given by

$$Y = \frac{\left[2 + \frac{a}{W}\right]}{B\sqrt{W}\left[1 - \frac{a}{W}\right]^{3/2}} \left[0.886 + 4.64\,\frac{a}{W} - 13.32\left[\frac{a}{W}\right]^2 + 14.72\left[\frac{a}{W}\right]^3 - 5.6\left[\frac{a}{W}\right]^4\right], \tag{2}$$

depending on the actual crack length a, the material thickness B, and the length of the specimen W.

Both, a change of the crack length (i) or crack closure (ii) influences the geometry factor Y. These dependencies are illustrated by the consideration of a standard C(T) specimen without residual stresses:

(i) The change of Y depending on the crack length is given by Eq. (2).
(ii) Negative applied forces lead to the occurrence of crack closure along the entire fracture surface. Thus, SIF and Y are set to zero.

In the following, a change of the linear relation between applied load and SIF, as given by the geometry factor Y, is interpreted as a change of the crack geometry, where the same applied loads lead to different stress distributions in the specimen depending on the crack geometry, resulting in different SIFs. Thus, the term *crack geometry* is used to describe the linear correlation between applied loading and resulting SIF. The meaning of the term *crack geometry* is also used in a similar way for three-dimensional problems in the following sections.

Eqs. (1) and (2) give a single SIF for the entire crack front due to mode I crack opening of sheet like materials without consideration of crack closure effects; however, high compressive residual stresses may lead to complex crack closure mechanisms, which violate the assumption of an opened crack front in Eq. (2).

2.2. Numerical SIF calculation based on the crack closure technique

In the following, a three-dimensional problem with a one-dimensional crack front is considered, which accounts for the complex residual stress field. The crack front is assumed to be perpendicular to the material surface and the SIFs depend on the position along the crack front. Thus, SIFs next to the surfaces differ from SIFs next to the mid-thickness of the material. The gradient of SIFs along the crack front increases when residual stress gradients are present. Therefore, this work distinguishes between an averaged SIF K_{avg} and a local depth-depend SIF K_{local}, which represents the SIF at a specific location along the crack front. In this work, K_{avg} is calculated based on the element-wise determined SIF K_{ele} via a finite element (FE) model to take the residual stress gradient into account

$$K_{avg} = \frac{\sum_{J=1}^{N_{ele}} b_{ele}^{J} K_{ele,J}}{\sum_{J=1}^{N_{ele}} b_{ele}^{J}}, \tag{3}$$

where N_{ele} is the number of elements and b_{ele}^{J} is the element thickness of the Jth element along the crack front, which is directed in the z-direction of the applied FE model. Note, that the difference of SIFs based on Eqs. (1) and (2) and K_{avg} are negligible for a residual stress-free C(T) specimen in this work.

An energy based approach, the crack closure method or two-step crack closure technique, is used to numerically determine the local SIF. The crack is extended element-wise in the applied approach, by releasing the nodes of the crack front from the previous increment. The interested reader is referred for a detailed description of this technique to [23,24]. The elemental energy release rate G_{ele}^{J} of the J^{th} element is calculated via

$$G_{ele}^{J} = \frac{1}{2\, b_{ele}^{J}\, \Delta a} \sum_{l=1}^{2} C^{l}\, u_{y}^{l}\, F_{y}^{l} = \sum_{l=1}^{2} G_{node}^{*,l}, \tag{4}$$

where Δa represents the increment of the crack length extension, F_{y}^{l} the nodal force, u_{y}^{l} the nodal displacement, l the local node number, and C^{l} a weighting parameter. C^{l} takes the size of the new surface due to the crack extension after releasing the nodes at crack front from the previous increment into account:

$$C^{1} = \frac{b_{ele}^{J}}{b_{ele}^{J} + b_{ele}^{J-1}}, \quad C^{2} = \frac{b_{ele}^{J}}{b_{ele}^{J+1} + b_{ele}^{J}}, \tag{5}$$

see Fig. 1.[1] The energy release rate related to each element G_{ele}^{J} consists of the contributions $G_{node}^{l,*}$ calculated for the respective node values F_y and u_y. Two distinctions depending on the sign of F_y and u_y are made regarding $G_{node}^{l,*}$, leading to four different cases

$$G_{node}^{l,*} = \begin{cases} -G_{node}^{l} = G_{node,sep}, & \text{for} \quad F_y \leqslant 0;\ u_y \geqslant 0, \\ G_{node}^{l} = G_{node,pen}, & \text{for} \quad F_y \geqslant 0;\ u_y \leqslant 0, \\ 0, & \text{for} \quad F_y > 0;\ u_y > 0, \\ 0, & \text{for} \quad F_y < 0;\ u_y < 0 \end{cases} \quad \text{with} \quad G_{node}^{l} = \frac{C^{l}\, u_{y}^{l}\, F_{y}^{l}}{2\, b_{ele}\, \Delta a}. \tag{6}$$

$u_y \geqslant 0$ represents a physically opened crack, corresponding to a separation of nodes, leading to a positive SIF. The energy release rate for $u_y \geqslant 0$ is named $G_{node,sep}$. However, $u_y < 0$ leads to penetration of crack surfaces, which does not occur at real cracks [2]. The energy

[1] Note, that the sum of C^1 and C^2 for adjacent elements in the same node is one: $C_{ele,n}^{2} + C_{ele,n+1}^{1} = \frac{b_{ele}^{n}}{b_{ele}^{n+1} + b_{ele}^{n}} + \frac{b_{ele}^{n+1}}{b_{ele}^{n+1} + b_{ele}^{n+1-1}} = 1$.
[2] Note, that $u_y < 0$ does not occur, if penetration is prevented via modelling crack face contact.

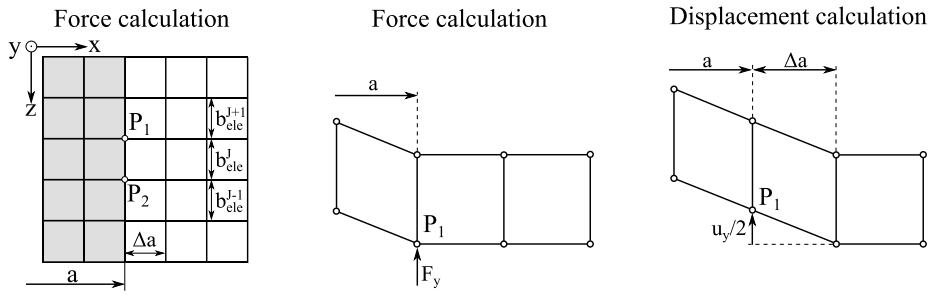

Fig. 1. Schematic of the calculated nodal forces F_y^l and the displacements u_y^l in point P_1 and P_2 along the one-dimensional crack front.

release rate in case of $u_y < 0$ is named $G^l_{node,pen}$. The penetration of crack surfaces is mathematically taken into account, by linking $G^l_{node,pen}$ to a negative SIF:

$$K_{ele} = \begin{cases} \sqrt{E' \left| G^l_{node,sep} - G^l_{node,pen} \right|}, & \text{for} \quad |G^l_{node,sep}| - |G^l_{node,pen}| \geqslant 0, \\ -\sqrt{E' \left| G^l_{node,sep} - G^l_{node,pen} \right|}, & \text{for} \quad |G^l_{node,sep}| - |G^l_{node,pen}| < 0 \end{cases}, \tag{7}$$

where E' represents the modified Young's modulus, i.e. for plane stress $E' = E$ or for plane strain $E' = E(1-\nu^2)^{-1}$ with Poisson's ratio ν. A negative SIF is treated as pure mathematical value in terms of SIF superposition. Special attention has to be paid when F_y and u_y have the same sign. These cases occur in residual stress fields with high gradients perpendicular to the surface (x–y plane). While a negative G_{node} is linked to an energy release rate, a positive G_{node} corresponds more to an energy storage. In this work, energy storage is considered as unphysical and therefore a positive G_{node} is set to zero instead. Finally, the average SIF over the crack front K_{avg} is calculated accordingly to Eq. (3).

2.3. Superposition principle of SIF

Based on linear elastic fracture mechanics, SIFs follow the superposition principle, see e.g. Withers [14]. Accordingly, a combined loading can be decomposed into different contributions, where each of the individual loadings can be applied to the structure separately. The resulting stresses and SIFs are determined from pure superposition of the stresses and SIFs resulting from the individual partial loadings, see Fig. 2(a). This principle is also applicable to components that include residual stresses. Thus, residual and applied stresses as well as SIFs are distinguished, where the residual SIF K_{res} is associated with residual stresses and the applied SIF K_{appl} with all applied loadings:

$$K_{tot} = K_{appl} + K_{res}. \tag{8}$$

Assuming that the crack geometry remain constant for the partial loadings which corresponds to an opened crack, K_{appl} can be calculated by Eq. (1) in a two-dimensional system. Two different methods are commomnly employed to calculate K_{res}, the weight function method [25,26] and the FE analysis [16,27].

This work discusses the influence of the crack geometry on the superposition principle and answers the question how K_{appl} and K_{res} would need to be calculated to apply the superposition principle consistently. The work is intended as proof of concept of the superposition principle even in the occurrence of compressive residual stresses, leading to a change of crack geometry due to crack closure mechanism.

3. SIF superposition in presences of high compressive residual stress fields demonstrated by FE analysis

In the following, an FE model is used to demonstrate the applicability of the superposition principle in case of high residual stress gradients and local crack closure effects.

3.1. Numerical model set up

As a case study, the applicability of the superposition is discussed based on the example of a C(T)100 specimen with 4.8 mm thickness and a complex residual stress field, e.g. generated by local modification techniques such as laser shock peening. In [28]

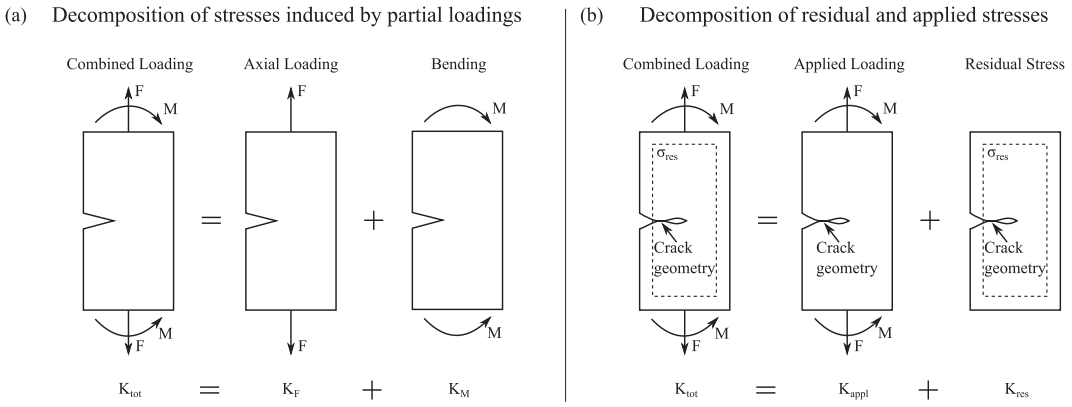

Fig. 2. The superposition principle of stresses allows the individual calculation of SIF for partial loading (K_F and K_M) to determine the total SIF K_{tot}, (a). The superposition principle can also be used to separate the SIF of residual and applied stresses (K_{res} and K_{appl}), (b). However, compressive residual stresses may influence the crack geometry by causing crack closure, which needs to be considered when the superposition principle is applied.

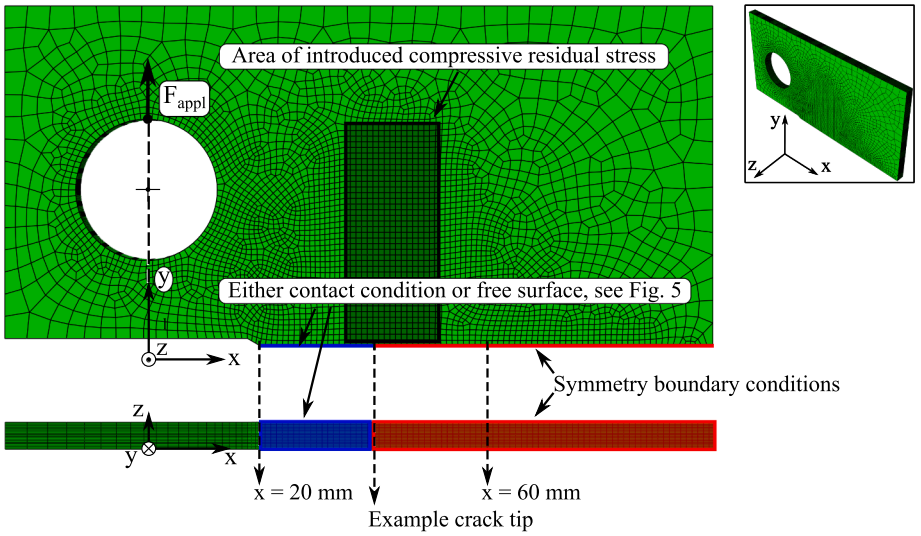

Fig. 3. FE model of a half C(T)100 specimen. Symmetry conditions are applied at the x–z symmetry plane in the uncracked region. These are replaced either by contact conditions to a rigid plate or by a free surface in the cracked area. Contact conditions simulate crack face contact in the case of combined loading. A free surface models a specific crack geometry of residual or applied loading; however, allows crack face penetration.

residual stresses with a compressive maximum of 300 MPa are introduced, representing approximately 85% of the yield strength of the investigated aluminium alloy AA2024. Based on the symmetry in the x–z plane of the problem, half of a C(T) specimen is modelled using the commercial FE software ABAQUS.[3] The FE model consists of approximately 100 000 three-dimensional eight-noded continuum elements with reduced integration (C3D8R). The element size along the fatigue crack path is $1 \times 1 \times 0.2\,\mathrm{mm}^3$, ensuring mesh independence and a high resolution of residual stress gradient in thickness direction. Linear elastic material behaviour is assumed with Young's modulus $E = 73$ GPa and Poisson's ratio $\nu = 0.33$, representative for aluminium alloys. The force F_{appl} is applied at the top nodes of the pin, where the pin is not explicitly modelled to avoid simulating contact between pin and C(T) specimen. Symmetry boundary conditions are applied along the symmetry plane before the crack growths. SIFs are calculated for different crack lengths based on the determined nodal force F_y and displacement u_y, as presented in Section 2.2. The crack is extended node-wise along the crack path by replacing the symmetry conditions at the nodes by either contact conditions to a rigid plane or a free surface. The crack front is modelled straight along the z-direction. The assumption of a crack extension along the symmetry plane and a straight crack front are proven by an *experimental simulation* for laser-shock-peening-introduced residual stresses in AA2024 regarding the FCGR

[3] It should be noted, that symmetric through-the-thickness residual stress profiles allow the use of symmetry conditions along the x–y plane at the mid-thickness of the material as well. However, application of laser shock peening from both sides, may lead to an unsymmetric through-the-thickness residual stress profile; hence, possible through-the-thickness symmetric simplifications are neglected.

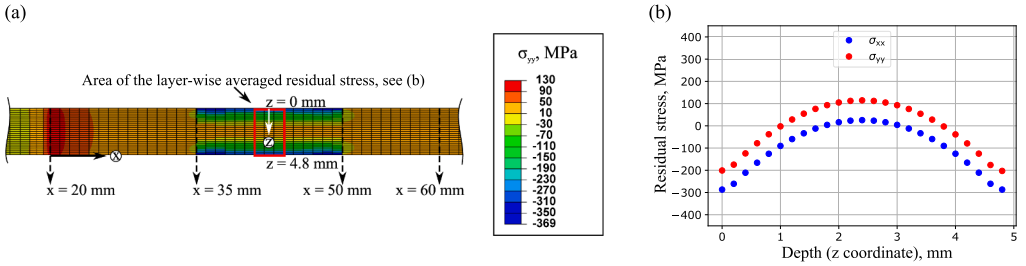

Fig. 4. Residual stress distribution at the symmetry plane of the C(T) specimen (a). Compressive residual stresses are present next to the surfaces at 35 mm $< x <$ 50 mm, balancing tensile residual stresses are present at mid-thickness and for $x <$ 35 mm as well as 50 mm $< x$. The residual stress profile over depth is shown in (b).

estimation [28]. The crack surface deforms due to formation of a new residual stress equilibrium after the crack extension. These assumptions need to be validated for the specific use cases; however, the general idea of the proposed SIF superposition can be applied for curved crack fronts as well.

Residual stresses are introduced by the eigenstrain approach [29,30], where the eigenstrains are modelled as thermal strains. For this purpose, anisotropic thermal expansion coefficients are assigned to certain regions of the C(T) specimen. The required thermal strain field is generated by a temperature increase, leading to the desired residual stress field.

The specific applied residual stress distribution in this study is related to a typical residual stress field after double-sided laser shock peening treatment, see Keller et al. [28]. Such a residual stress field is characterized by high compressive residual stresses next to the specimen surfaces and contains tensile residual stresses at mid-thickness, see Fig. 4. The specific residual stress distribution discussed in the following contains compressive residual stresses next to the surfaces at 35 mm $< x <$ 50 mm of the C(T) specimen. Balancing tensile residual stresses are present in front and behind the peened area. The specific considered residual stress distribution leads to complex crack closure phenomena at lower applied forces, as described in detail in [11]. Crack face contact occurs in regions of high compressive residual stresses next to the material surface at low applied forces, while the crack remains open at mid-thickness, where tensile residual stresses are located.

The eigenstrains of the laser-shock-peening-induced residual stresses correspond to the laser-shock-peening-introduced plastic strains. Thus, the plastic deformation due to the laser shock peening treatment is considered by the applied numerical simulation due to the introduced eigenstrains. It has to be mentioned, that the source of the eigenstrains does not need to be laser shock peening, e.g. plastic deformation induced by the plastic wake could be introduced to the model as well, as long as the corresponding plastic deformation is known. As the plastic wake depends mainly on the maximum SIF of a load cycle and the material yield strength, correction functions of SIFs calculated without the consideration of the plastic wake can be found. However, the determination of a correction function is not practical for nearly arbitrary plastic strain profiles introduced by processes such as laser shock peening. Preliminary simulations of the authors showed, that the contact forces at the crack surfaces as well as the residual stress redistribution do not lead to plastic deformation that influence the SIF significantly. Thus, the elastic simulations includes the effect of the laser-shock-peening-induced plastic deformation as eigenstrains of the residual stress field.

3.2. *Proof of concept: SIF superposition considering the specific crack geometry*

The described FE model of a C(T) specimen is used to demonstrate the importance of the changed crack geometry due to crack closure, to calculate the residual and applied SIF by numerical simulation separately, see Fig. 5. Firstly, the SIF K_{comb}, the nodal displacements $u_{y,comb}$ and the nodal forces $F_{y,comb}$ at the crack front are calculated for combined loading with crack face contact. Additionally, the crack geometry is recorded, i.e. the nodes along the crack surfaces which are in crack face contact. Secondly, the crack extension simulations are performed without the modelling of crack face contact and either with present residual or applied stresses, described as separated loading. Symmetry boundary conditions are applied at the nodes, which were in crack face contact for combined loading, to mimic the corresponding crack geometry. The individual simulations of applied and residual stresses give the applied SIF K_{app}^{FE,Y^*} and the residual SIF K_{res}^{FE,Y^*} for the specific crack geometry of the combined loading indicated by the specific geometry factor Y^* calculated by the FE analysis. Furthermore, the corresponding nodal displacements and forces are stored as well ($u_{y,app}$, $u_{y,res}$, $F_{y,app}$, and $F_{y,res}$). The total nodal displacement $u_{y,tot}$, forces $F_{y,tot}$ and the total SIF $K_{y,tot}$ are calculated by the superposition of the respective quantities for separate loading.

Following this described simulation scheme, SIF, u_y, and F_y are calculated separately for applied and residual stresses at two applied forces, i.e. $F_{appl} = 400$ N and $F_{appl} = 4000$ N. $F_{y,comb}$ and $u_{y,comb}$ are shown for the respective crack length over the depth of the C(T) specimen in Fig. 6. $|F_{y,tot} - F_{y,comb}|$ and $|u_{y,tot} - u_{y,comb}|$ indicate the respective absolute error, which are less than one per mill in relative terms.

Fig. 6(h) indicates a closed crack front at regions of high compressive residual stresses, as $u_{y,comb} = 0$ mm and $F_{y,comb} \geqslant 0$ N. It has to be mentioned, that negative forces $F_{y,comb}$ do not lead to a negative SIF, when crack face contact is modelled, as $u_{y,comb} = 0$ mm holds. While crack face contact occurs for $F_{appl} = 400$ N, no crack closure can be observed for $F_{appl} = 4000$ N.

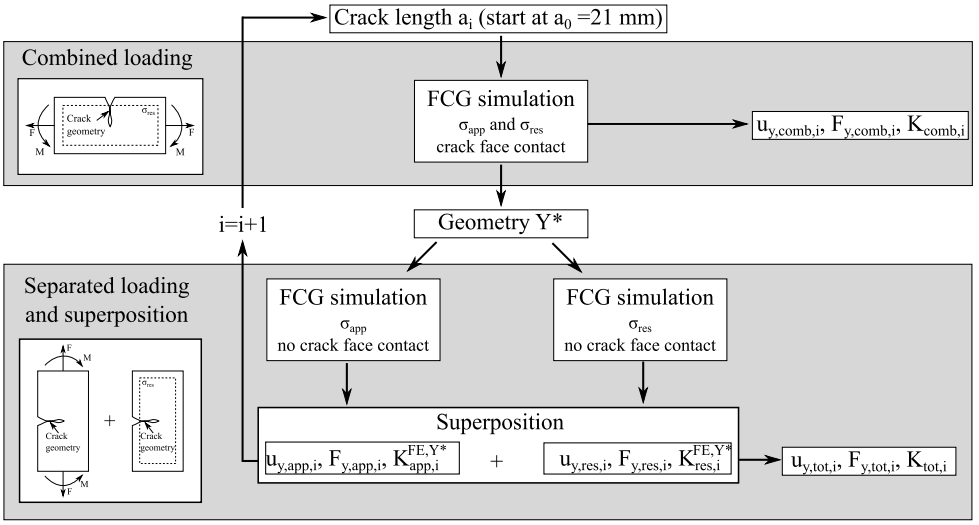

Fig. 5. Schematic of the simulation approach to demonstrate the application of the superposition principle. An FE simulation is used to calculate the crack geometry, indicated by Y^*, the nodal displacements $u_{y,comb}$, and forces $F_{y,comb}$ for the combined load case. The respective SIF K_{comb} is calculated subsequently based on $u_{y,comb}$ and $F_{y,comb}$. $a_0 = 21$ mm is the starting crack length of the simulation. Subsequently, $u_{y,appl/res}$ and $F_{y,appl/res}$ caused by applied and residual stresses considering the specific crack geometry Y^* are calculated separately. The SIF $K_{app}^{FE,Y*}$ and $K_{res}^{FE,Y*}$, calculated by the respective nodal displacements and forces, are superimposed to calculate the total SIF K_{tot}.

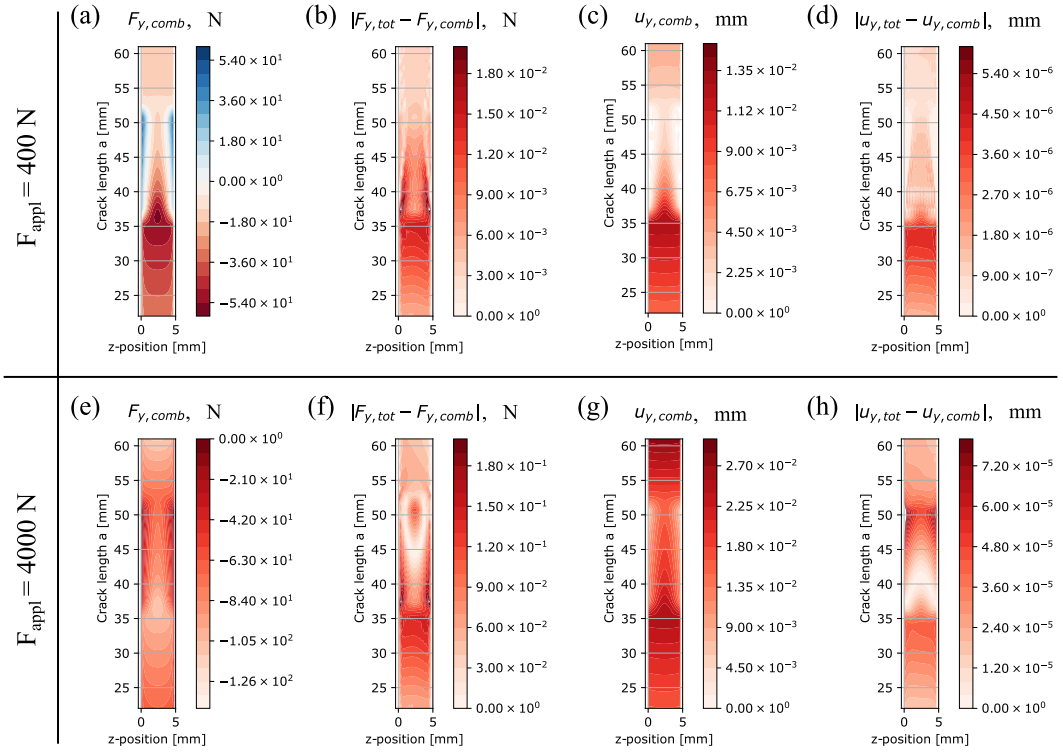

Fig. 6. Nodal force F_y and displacement u_y at the respective crack front for combined loading with $F_{appl} = 400$ N (a,c) and $F_{appl} = 4000$ N (e,g). The absolute error of the superposition is calculated by $F_{err} = \left|F_{y,tot} - F_{y,comb}\right|$ and $u_{err} = \left|u_{y,tot} - u_{y,comb}\right|$ for the nodal forces and displacements at $F_{appl} = 400$ N (b,d) and $F_{appl} = 4000$ N (f,h).

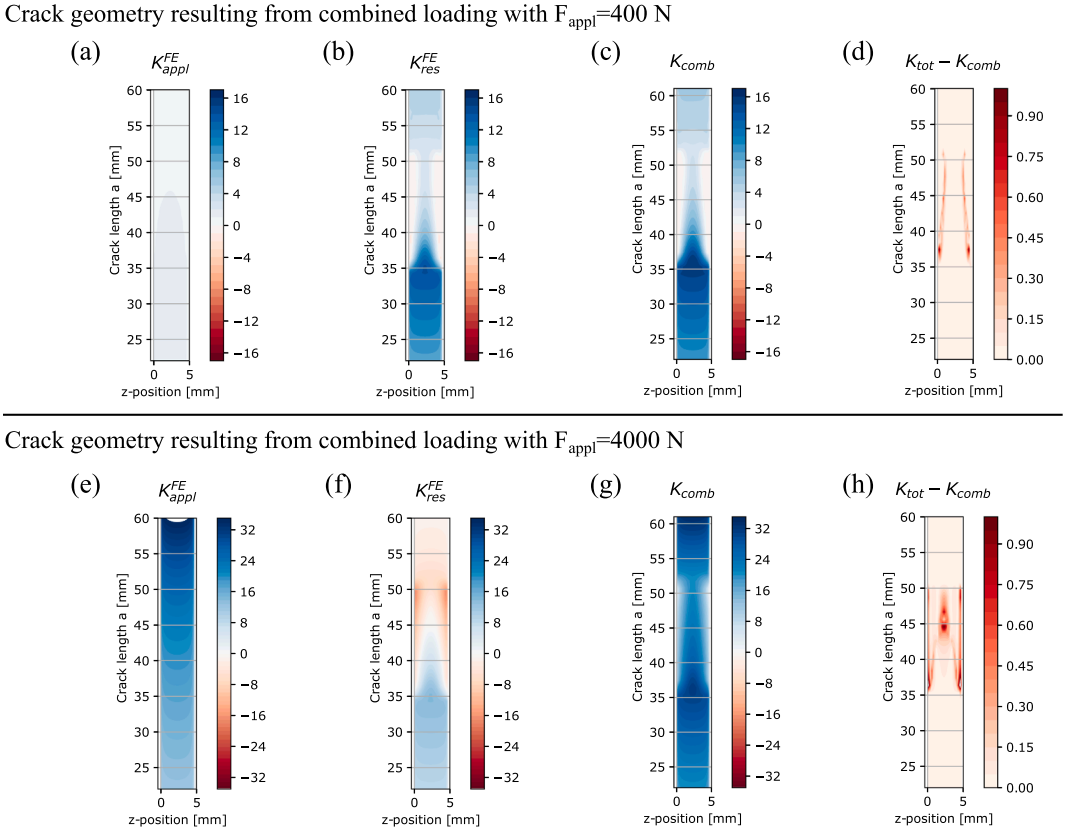

Fig. 7. Local SIFs over depth for crack length 22 mm $< a <$ 60 mm. K^{FE}_{appl} and K^{FE}_{res} are calculated for the respective crack geometry resulting from the combined loading with $F_{appl} = 400$ N (a,b) and $F_{appl} = 4000$ N (e,f). The SIF K_{comb} of the combined loading is shown in (c) and (g) for the respective applied force. The error of the superposition of K^{FE}_{res} and K^{res}_{appl} remains below 1 MPa$\sqrt{\text{m}}$, except for regions which show to a positive energy release rate, see (d) and (h).

The superposition of the SIF over depth is shown for every crack length in in Fig. 7 and in a two-dimensional plot as example for carachteristic crack lengths in Fig. 8 at $F_{appl} = 400$ N and $F_{appl} = 4000$ N. The penetration of the crack edges[4] allows the calculation of negative SIF, as present for K^{FE}_{res} at $F_{appl} = 4000$ N. It has to be mentioned, that a negative residual SIF does not have a physical interpretation, but reduces the total SIF after superposition. The change of the crack geometry by crack closure under combined loading prevents the occurrence of a negative total SIF K_{tot}. The superposition of K^{FE}_{appl} and K^{FE}_{res} has an overall small error, see Fig. 7(d) and Fig. 7(h). The error increases, when a sign change is present for K^{FE}_{res}, see also Fig. 8(c). This increased error is caused by the fact that the energy release rate is set to zero in case of nodal value pairs u_y and F_y having the same sign, see Eq. (6). Crack face contact in regions of high compressive residual stresses causes a reduced K_{comb} for $x > 50$ mm and $F_{appl} = 400$ N, see Fig. 7. The area of crack face contact has not to been connected to the crack front.

A closer look on the SIFs along the crack front, Fig. 8, illustrates the effect of the changed geometry depending on the combined loading. The crack is completely opened in front the peened area for $F_{appl} = 4000$ N Fig. 8(a) and $F_{appl} = 400$ N Fig. 8(b); hence, the residual SIF is the same. Crack closure effects occur at $F_{appl} = 400$ N inside the peened area Fig. 8(d) and lead to a zero value residual SIF next to the material surfaces, but a positive SIF at mid-thickness, where tensile residual stresses are located. The force $F_{appl} = 4000$ N opens the crack completely Fig. 8(c), so that the residual SIF is negative in the region of compressive residual stresses next to the material surface, as the crack geometry allows the penetration of the crack surface. The residual stresses at mid-thickness is set to zero, as the nodal value pairs u_y and F_y have the same sign, when the energy release rate is calculated. This leads to a slight mismatch of K_{comb} and K_{tot}, which does not have a significant impact on averaged SIFs $K_{comb,avg}$ and $K_{tot,avg}$. Crack closure still occurs at $F_{appl} = 400$ N inside the peened area, even when the crack front is already located behind the peened area. In contrast, $F_{appl} = 4000$ N opens the crack completely. Consequently, the residual SIF for the crack geometry at $F_{appl} = 4000$ N and $F_{appl} = 400$ N differ, see Fig. 8 (e) and (f). Note, that the linear relation between the force F_{appl} and the applied SIF differs for the regions inside and behind the peened

[4] The penetration of crack edges is allowed for the individual calculation of K^{FE}_{res} and K^{FE}_{appl}, see Fig. 5.

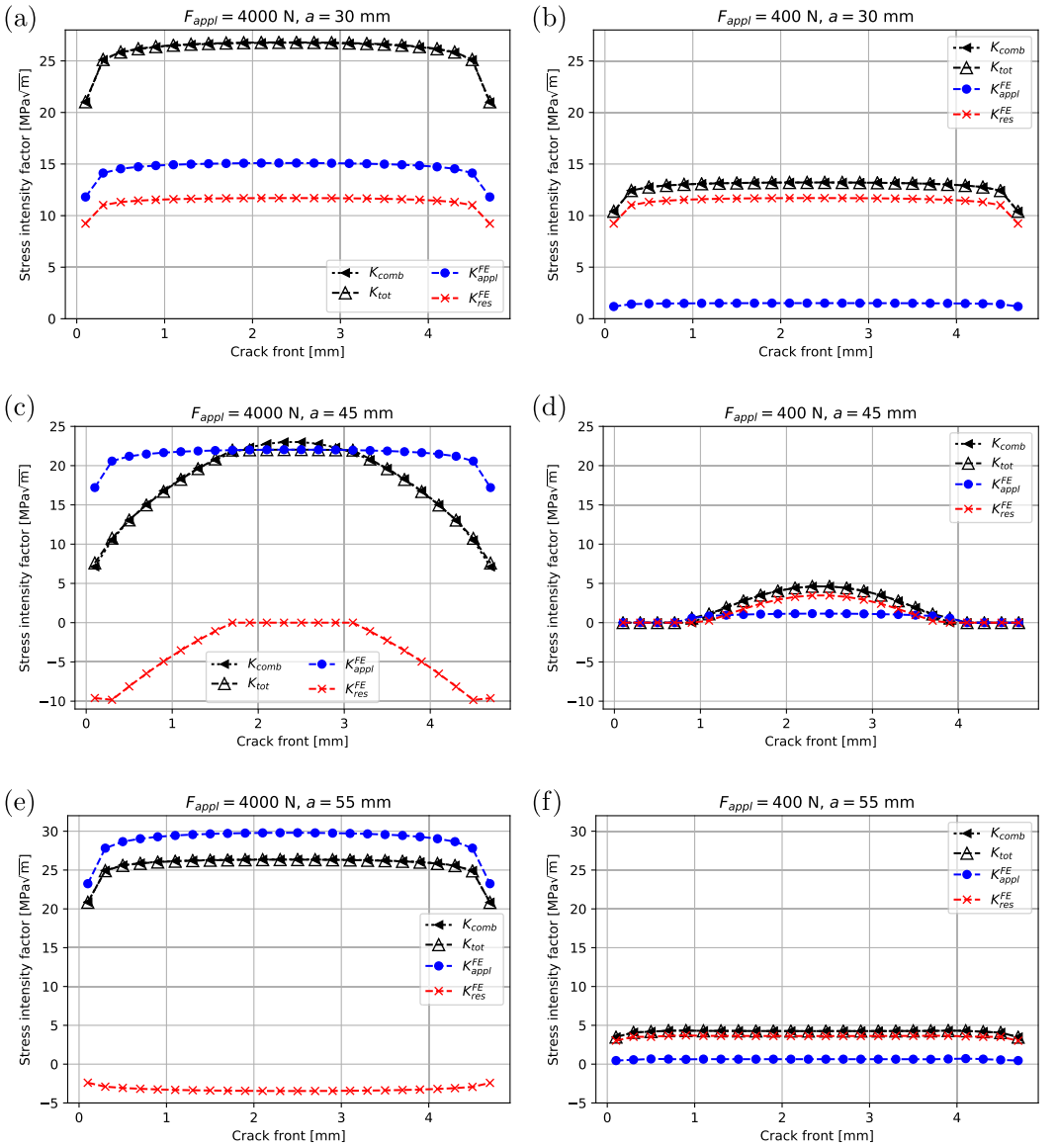

Fig. 8. SIFs along the crack front for the crack lengths $a = 30$ mm (a,b), $a = 45$ mm (c,d), and $a = 55$ mm (e,f) at the applied forces $F_{appl} = 400$ N and $F_{appl} = 4000$ N. While nearly constant tensile through-the-depth residual stresses cause an approximately constant SIF distribution in front (a,b) and behind (e,f) the peened area, compressive residual stresses next to the material surface and tension at mid-thickness cause a curved SIF distribution inside the peened area (c,d). The specific crack geometry resulting from crack closure effects cause different residual SIF distributions along the crack front inside and behind the peened area for different applied loads. In contrast, the residual SIF distribution is the same in front of the peened area, as the crack is completely opened at $F_{appl} = 400$ N and $F_{appl} = 4000$ N.

area for the geometry at $F_{appl} = 400$ N as well, while this linear relation is the same for the complete opened crack at $F_{appl} = 4000$ N.

Although small differences of K_{tot} and K_{comb} can be observed at locations, where the sign of the residual stress changes, the averaged SIF $K_{tot,avg}$ and $K_{comb,avg}$ coincide, see Fig. 9(a). In this regard, the general applicability of the superposition in case of complex crack closure behaviour, caused by residual stresses with high gradients over the material thickness, is clarified by considering crack closure as a change of the crack geometry.

The applied SIF depend on the crack geometry at combined loading, see Fig. 9(b). The crack is completely opened at $F_{appl} = 4000$ N; hence, the geometry factor of the combined loading corresponds to the assumptions of Eq. (2). Thus, $K^{FE}_{appl,avg}$ agrees to $K^{ASTM}_{appl,avg}$, where $K^{ASTM}_{appl,avg}$ is calculated based on ASTM, see Eqs. (1) and (2). However, crack closure occurs at $F_{appl} = 400$ N, leading to a different geometry factor compared to a completely opened crack as assumed by applying ASTM: $K^{FE}_{appl,avg} < K^{ASTM}_{appl,avg}$. This difference

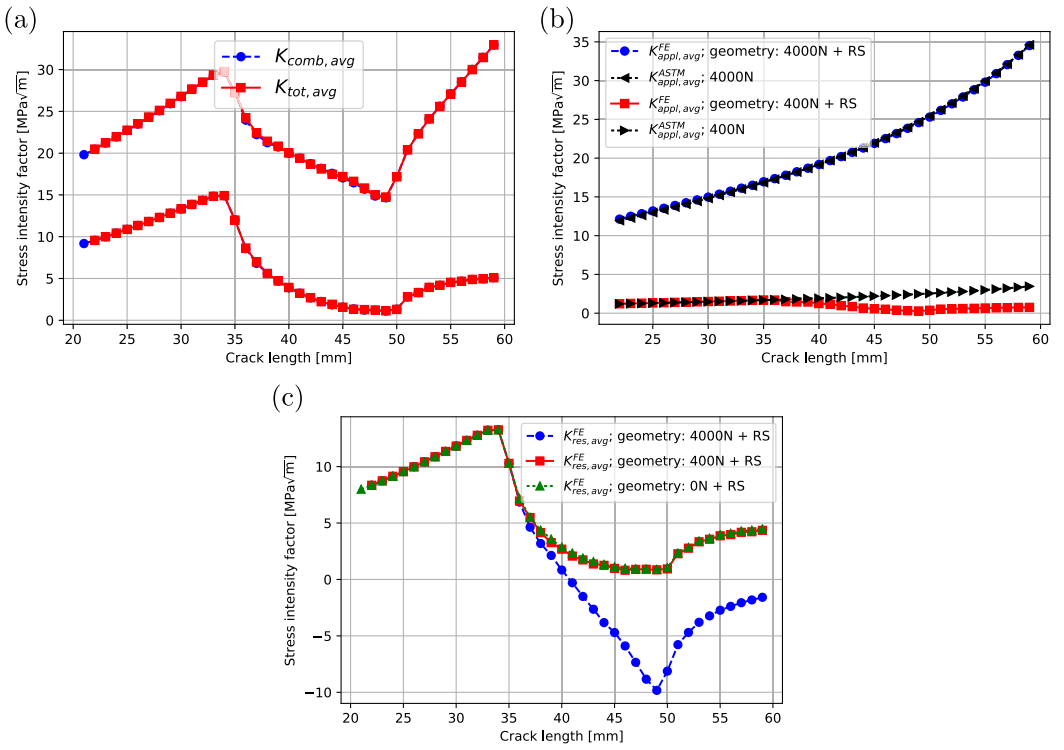

Fig. 9. Comparison of SIF determined by FE simulations for combined loading $K_{comb,avg}$ and after superposition $K_{tot,avg}$ for $F_{appl} = 400\,\mathrm{N}$ and $F_{appl} = 4000\,\mathrm{N}$ (a). $K^{FE}_{appl,avg}$ and $K^{FE}_{res,avg}$ determined for different crack geometries under combined loading as well as $K^{ASTM}_{appl,avg}$ calculated for applied loading only (b) and (c). RS refers to residual stress in the graphs.

shows that the analytical calculation according to ASTM, i.e. $K^{ASTM}_{appl,avg}$ does not calculate the applied SIF accurately when crack closure occurs.

The residual SIF is calculated for the geometry of combined loading for different applied loadings, see Fig. 9(c). The crack is completely opened for $F_{appl} = 4000\,\mathrm{N}$. Thus, penetration of the fracture surfaces is allowed along the entire crack for the calculation of $K^{FE}_{res,avg}$ corresponding to the geometry of an opened crack. The penetration of crack edges leads to negative $K^{FE}_{res,avg}$. In contrast, $F_{appl} = 400\,\mathrm{N}$, and $F_{appl} = 0\,\mathrm{N}$ do not open the crack completely during combined loading, leading to crack face contact. In this specific case, the areas of crack face contact are nearly identical resulting in the approximately same crack geometry. Consequently, $K^{FE}_{res,avg}$ is almost identical for $F_{appl} = 400\,\mathrm{N}$ and $F_{appl} = 0\,\mathrm{N}$. $K^{FE}_{res,avg}$ does not become negative, due to the specific crack geometry.

This investigation demonstrates that both, the residual as well as the applied SIF depend on the crack geometry under combined loading. This dependency has to be taken into account, when residual stress modification techniques are applied to modify K_{comb}, as the efficiency of such modification techniques depend on the applied loading.

4. Discussion of SIF superposition for practical application

4.1. Different SIF definitions

Besides the previous discussion and illustration of the superposition principle in terms of $K_{appl,avg}$ and $K_{res,avg}$ considering the geometry under combined loading, two different definitions of the residual SIF $K_{res,avg}$ are theoretical possible simplifying the practical application by changing the physical meanings of either $K_{res,avg}$ or $K_{appl,avg}$. All three definitions are discussed in the following:

1. SIF superposition following stress superposition.
   $K_{appl,avg}$ and $K_{res,avg}$ are separated by a superposition principle of stresses, as described in Section 3. This means that K_{res} is the SIF caused by residual stresses at specific applied loading. However, this definition requires the exact knowledge of the crack geometry, e.g. described by Y, at combined loading to calculate $K_{appl,avg}$ and $K_{res,avg}$ independently.
2. $K_{res,avg}$ as difference to residual stress–free material.
   $K_{res,avg}$ is taken as difference between $K_{comb,avg}$ and $K_{appl,avg}$, where $K_{appl,avg}$ is calculated for residual stress-free material, e.g. based

on standard $K^{ASTM}_{appl,avg}$, $K_{res,avg} := K_{comb,avg} - K^{ASTM}_{appl,avg}$. This definition is for instance used by Bao et al. [25] and has its origin in the consideration of tensile residual stresses. By using this concept for cases including crack closure, K_{res} describes the SIF change compared to residual stress-free material. Thus, K_{res} depends on the applied loading, which influences the crack geometry as discussed in the previous section.

3. $K_{res,avg}$ as residual SIF.

   $K_{appl,avg}$ is defined as difference between $K_{comb,avg}$ and $K_{res,avg}$, where $K_{res,avg}$ is calculated without external loadings, i.e. $K^{0\,\mathrm{N}}_{res,avg}$ is calculated at $F_{appl} = 0\ N$ and used to calculate the applied SIF: $K_{appl,avg} := K_{comb,avg} - K^{0\,\mathrm{N}}_{res,avg}$. This definition uses the original meaning of *residual* and *applied*. $K_{res,avg}$ is the SIF, which remains in the material after all external loadings are removed ($F_{appl} = 0$ N); hence, K_{res} is the residual SIF and does not depend on the applied loading.

While the first definition represents the mathematically correct application of the superposition principle of stresses in the sense of stress superposition in an elastic body with small deformations, the second definition allows an easy calculation of $K_{appl,avg}$ and has its strength in the calculation of SIF in completely opened cracks. The third definition allows the natural description of the material in subsequent application, as the residual SIF is considered as initial state.

4.2. Applicability of SIF superposition definitions

The consequences of the proposed SIF definition of the previous section are addressed in the following by consideration of averaged SIF, see Eq. (3). The physical meaning of the residual and applied SIF based from the individual SIF definition, their practical use, and the consequences on the specific calculation are discussed.

For this purpose, the same residual stress distribution as before, i.e. Fig. 4, is considered. In this regard, tensile residual stresses are present for 20 mm $< a <$ 35 mm as well as for 50 mm $< a <$ 60 mm and compressive residual stresses at 35 mm $\leqslant a \leqslant$ 50 mm. The tensile residual stresses lead to an opened crack even without applied loading $F_{appl} \geqslant 0$ N at 20 mm $< a <$ 35 mm. Thus, the crack geometry of combined and applied loading as well as the crack geometry with residual stresses represents always an opened crack. As the crack geometry is the same for these loading conditions, the calculated SIFs according to all three definitions are the same, see Fig. 10. Thus, the distinction of the three definitions does not influence the commonly used SIF superposition for tensile residual stresses and tensile loadings in the literature.

In contrast to tensile residual stresses, compressive residual stresses combined with tensile loading lead to different SIFs according to the SIF definitions. Two characteristic cases in terms of the crack geometry are discussed in the following to demonstrate the effect of compressive residual stresses, i.e. the discussion concentrates on a crack within 35 mm $\leqslant a <$ 60 mm according to Fig. 3 and 4. The first case represents the situation of a completely opened crack, which is present at combined loading for $F_{appl} = 4000$ N, see Section 3. The second case considers an applied loading of $F_{appl} = 400$ N, where the crack geometry under combined loading approximately corresponds to the crack geometry resulting from residual stresses only.

The applied and residual SIFs of Definition 2 correspond to Definition 1 considering the opened crack geometry at $F_{appl} = 4000$ N, see Fig. 10(a) and (b). The completely opened crack under combined loading allows the calculation of the applied SIF according to ASTM, i.e. Eq. (1) and (2), which also holds for Definition 1. For Definition 1 and 2, the residual SIF is calculated by allowing the penetration of the entire crack surface, leading to $K^{Dif.1}_{res,avg} < 0$ MPa$\sqrt{\mathrm{m}}$ and $K^{Dif.2}_{res,avg} < 0$ MPa$\sqrt{\mathrm{m}}$. Definition 3 considers the residual SIF as SIF without external loading; hence, the residual SIF is calculated with the assumption of crack face contact. This leads to a residual SIF $K^{Dif.3}_{res,avg} \geqslant 0$ MPa$\sqrt{\mathrm{m}}$. Thus, the applied SIF differs from the applied SIF of Definition 1 and 2, see Fig. 10(b).

In contrast to $F_{appl} = 4000$ N, the crack partially closes for combined loading at $F_{appl} = 400$ N. Therefore, the applied and residual SIF of Definition 1 and Definition 3 are in a good agreement [5]. It is important to note, that the applied SIF changes depending on the closure for Definition 1 and 3, see Fig. 10(c).

To conclude, all definitions of the superposition principle give the same total SIF, see Fig. 10(e). While the partition in residual and applied SIF is the same for all three definitions considering tensile residual stresses and tensile loading, residual and applied SIF differ depending on the definition when compressive residual stresses are present. Definition 1 calculates the residual and applied SIF depending on the source of the respective stresses. Definition 2 assumes that the applied SIF is not influenced by residual stresses and corresponds to Definition 1, as long as the crack is completely opened. Thus, Definition 2 is practically applicable, when external forces open the crack completely. The residual SIF needs to be calculated once with assumption of crack face penetration, thereafter the applied SIF can be calculated with standard equations, like ASTM, to determine the total SIF for different external loadings. The residual SIF of Definition 2 describes the change of the total SIF compared to residual stress-free material in any case. Thus, the residual SIF of Definition 2 can be easily linked to changes of the fatigue behaviour due to residual stresses. Definition 3 calculates the residual SIF as remaining SIF without external loading. Under decreasing external loading the SIF of Definition 1 and 3 match. Additionally, when the external loading is zero, SIFs of the two Definitions 1 and 3 are identical. The residual SIF by Definition 3 is of importance, when the permanent loading of a crack has to be evaluated. The residual SIF of Definition 3 is calculated by considering crack closure along the entire crack surface. Note, that residual and applied SIFs of different definitions cannot be mixed to calculate the total SIFs under compressive residual stresses.

[5] The applied and residual SIF of Definition 1 and 3 are the same when the areas of crack closure are the same, i.e. at $F_{appl} = 0$ N.

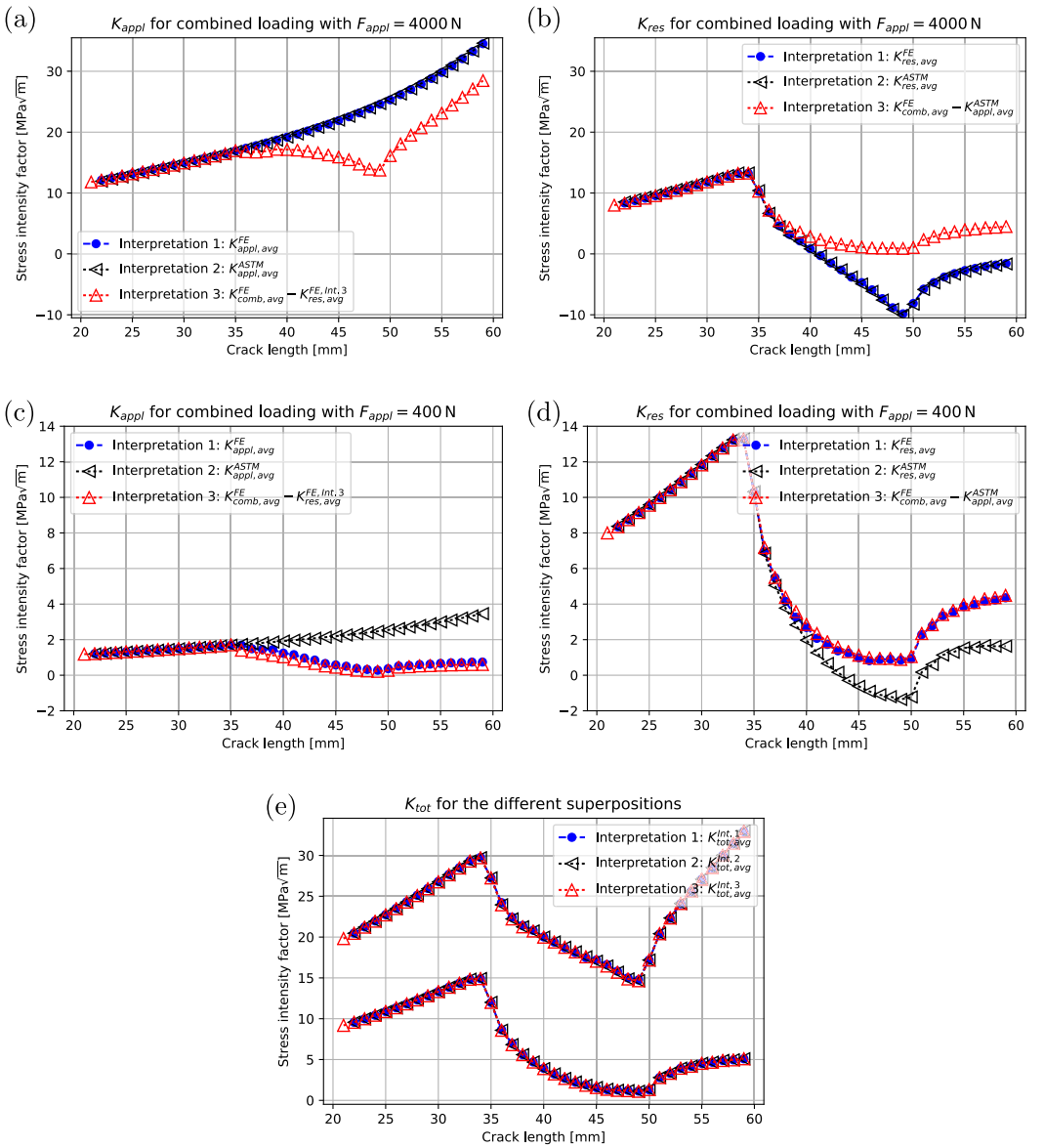

Fig. 10. SIF corresponding to the three proposed definitions for $F_{appl} = 4000$ N (a,b) as well as for $F_{appl} = 400$ N (c) and (d). The two applied forces lead to characteristic cases, where Definition 2 coincides with Definition 1 for an completely opened crack (a,b) and Definition 1 corresponds to Definition 3 at low applied forces (c,d). The addition of the respective residual and applied SIF according to its definition leads to the same SIF of the combined loading (e).

Finally, a short comment on FCG: (i) the assumption, that the total SIF range of combined loading (generally known as ΔK_{tot})[6] is not influenced by residual stresses does not hold for a general case. The residual SIF changes depending on the crack geometry as demonstrated in Section 3. The assumption of an unchanged total SIF range ΔK_{tot} can be made when the crack geometry remains unchanged for the minimal and maximal applied loading. (ii) A simplification of the residual SIF calculation can be made, when the maximum applied loading opens the crack completely and the minimum applied loading causes a crack geometry approximately corresponding to a closed crack. The residual SIF at maximum loading can be calculated with allowing the penetration of the crack surfaces and the residual SIF at minimum loading can be approximated by applying crack face contact.

[6] ΔK is the difference of the SIF at minimum and maximum externally applied load of a load cycle.

5. Conclusion

This work demonstrates the applicability of the superposition principle of SIF considering high compressive residual stresses and crack closure phenomena, where crack face contact is considered as a change of crack geometry. The specific crack geometry under combined loading of residual and applied stresses has to be known to apply the superposition of SIF according to the superposition of stresses in an elastic body with small deformation. Considering a given residual stress distribution, the applied loadings define the occurrence of crack closure. As the crack geometry changes with the occurrence of crack closure, the partition of the total SIF into the residual and applied SIF changes as well. Two alternative definitions of applied and residual SIF are proposed, leading to different physical meanings of the respective SIF. These definitions simplify the correlation between changes of applied and residual SIF to resulting physical phenomena such as FCG. The different definitions coincides with the SIF calculated by the superposition of stresses for the characteristic cases of an completely opened and nearly closed crack. All three definitions of SIF match for the case of tensile residual and applied stresses and fit to the commonly applied superposition principle of SIFs in tensile residual stress fields.

Declaration of Competing Interest

The authors declare that they have no known competing financial interests or personal relationships that could have appeared to influence the work reported in this paper.

References

[1] Garcia C, Lotz T, Martinez M, Artemev A, Alderliesten R, Benedictus R. Fatigue crack growth in residual stress fields. Int J Fatigue 2016;87:326–38.
[2] Servetti G, Zhang X. Predicting fatigue crack growth rate in a welded butt joint: the role of effective R ratio in accounting for residual stress effect. Eng Fract Mech 2009;76:1589–602.
[3] Lados DA, Apelian D. The effect of residual stress on the fatigue crack growth behavior of Al-Si-Mg cast alloys. Mech Corrective Math Models Metallurg Mater Trans A 2006;37:133–45.
[4] Baptista R, Infante V, Branco C. Fully dynamic numerical simulation of the hammer peening fatigue life improvement technique. Procedia Eng 2011;10:1943–8.
[5] Mutoh Y, Fair G, Noble B, Waterhouse R. The effect of residual stresses induced by shot-peening on fatigue crack propagation in two high strength aluminium alloys. Fatigue Fract Eng Mater Struct 1987;10:261–72.
[6] Kashaev N, Chupakhin S, Ventzke V, Horstmann M, Riekehr S, Barbini A, dos Santos JF, Keller S, Klusemann B, Huber N. Fatigue life extension of aa2024 specimens and integral structures by laser shock peening. In: MATEC web of conferences, vol. 165, EDP Sciences; 2018. p. 18001.
[7] Paris P, Erdogan F. A critical analysis of crack propagation laws. J Basic Eng 1963;85:528–33.
[8] NASGRO® Consortium and others, Fatigue crack growth computer program NASGRO® version 3.0. User manual, JSC-22267B, NASA Technical Report; 2001.
[9] Elber W. The significance of fatigue crack closure. In: Damage tolerance in aircraft structures, ASTM International; 1971.
[10] Newman JJ. A crack opening stress equation for fatigue crack growth. Int J Fract 1984;24:R131–5.
[11] Keller S, Horstmann M, Kashaev N, Klusemann B. Crack closure mechanisms in residual stress fields generated by laser shock peening: a combined experimental-numerical approach. Eng Fract Mech 2019;221:106630.
[12] Itoh Y, Suruga S, Kashiwaya H. Prediction of fatigue crack growth rate in welding residual stress field. Eng Fract Mech 1989;33:397–407.
[13] Parker A. Stress intensity factors, crack profiles, and fatigue crack growth rates in residual stress fields. In: Residual stress effects in fatigue. ASTM International; 1982.
[14] Withers P. Residual stress and its role in failure. Rep. Prog. Phys. 2007;70:2211.
[15] Newman JA, Smith SW, Seshadri BR, James MA, Brazill RL, Schultz RW, Donald JK, Blair A. Characterization of residual stress effects on fatigue crack growth of a friction stir welded aluminum alloy, National Aeronautics and Space Administration Langley Research Center Hampton, Virginia 23681-2199 NASA/TM2015-218685; 2015.
[16] Schnubel D, Huber N. The influence of crack face contact on the prediction of fatigue crack propagation in residual stress fields. Eng Fract Mech 2012;84:15–24.
[17] Liljedahl C, Brouard J, Zanellato O, Lin J, Tan M, Ganguly S, et al. Weld residual stress effects on fatigue crack growth behaviour of aluminium alloy 2024–T351. Int J Fatigue 2009;31:1081–8.
[18] LaRue J, Daniewicz S. Predicting the effect of residual stress on fatigue crack growth. Int J Fatigue 2007;29:508–15.
[19] Edwards L. Influence of residual stress redistribution on fatigue crack growth and damage tolerant design. In: Materials science forum. vol. 524, Trans Tech Publ; 2006. p. 363–72.
[20] Jones K, Dunn M. Fatigue crack growth through a residual stress field introduced by plastic beam bending. Fatigue Fract Eng Mater Struct 2008;31:863–75.
[21] Hill M, Kim J. Fatigue crack closure in residual stress bearing materials. In: Fatigue and fracture mechanics: 38th volume. ASTM International; 2012.
[22] Lam Y, Lian K. The effect of residual stress and its redistribution of fatigue crack growth. Theoret Appl Fract Mech 1989;12:59–66.
[23] Shivakumar K, Tan P, Newman Jr J. A virtual crack-closure technique for calculating stress intensity factors for cracked three dimensional bodies. Int J Fract 1988;36:R44–50.
[24] Krueger R. Virtual crack closure technique: history, approach, and applications. Appl Mech Rev 2004;57:109–43.
[25] Bao R, Zhang X, Yahaya NA. Evaluating stress intensity factors due to weld residual stresses by the weight function and finite element methods. Eng Fract Mech 2010;77:2550–66.
[26] Zhang Y, Ren X, Zhou J, Lu J, Zhou L. Investigation of the stress intensity factor changing on the hole crack subject to laser shock processing. Mater Des 2009;30:2769–73.
[27] Irving P, Ma YE, Zhang X, Servetti G, Williams S, Moore G, Dos Santos J, Pacchione M. Control of crack growth rates and crack trajectories for enhanced fail safety and damage tolerance in welded aircraft structures. In: ICAF 2009, bridging the gap between theory and operational practice. Springer; 2009. p. 387–405.
[28] Keller S, Horstmann M, Kashaev N, Klusemann B. Experimentally validated multi-step simulation strategy to predict the fatigue crack propagation rate in residual stress fields after laser shock peening. Int J Fatigue 2019;124:265–76.
[29] Hill MR. Modeling of residual stress effects using eigenstrain. In: ICF10, Honolulu (USA) 2001; 2001.
[30] Hu Y, Grandhi RV. Efficient numerical prediction of residual stress and deformation for large-scale laser shock processing using the eigenstrain methodology. Surf Coat Technol 2012;206:3374–85.